In situ speciation of actinides with a newly developed spectro-electrochemical cell

C. Hennig[1,2], J. Tutschku[2], A. Rossberg[1,2], G. Bernhard[2], A.C. Scheinost[1,2]

[1] The Rossendorf Beamline (BM20), ESRF, 38043 Grenoble, France
[2] Institute of Radiochemistry, Forschungszentrum Rossendorf eV, 01314 Dresden, Germany

Introduction

Natural aquatic and terrestrial environments exert large variations in redox state due to oxygen diffusion on one hand and microbial processes on the other hand. Actinides with their large number of oxidation states are especially susceptible to these redox changes, forming different aqueous complexes which may greatly differ by solubility and mobility. These complexes are often difficult to investigate due to their thermodynamic meta-stability. Therefore, we developed a new spectro-electrochemical cell, which allows to study the structure and speciation of aqueous actinide complexes *in situ* by X-ray absorption spectroscopy, while applying and maintaining a constant potential. Due to the specific safety requirements for handling of radioactive materials the electrochemical cell is gas tight. The spectro-electrochemical cell comprises two safety compartments and a special electrode arrangement. First U L_{III}-edge X-ray absorption spectra have been obtained from aqueous solutions of U(VI) and U(IV) in highly concentrated chloride solutions.

Electrochemistry

A drawing of the spectro-electrochemical cell is shown in Figure 1. The cell body consists of chemically resistant material (polytetrafluorethylene or polyvinylidenfluoride) and is sealed by two independent cover plates using rubber gaskets. These cover plates serve as double confinement against radionuclide release.

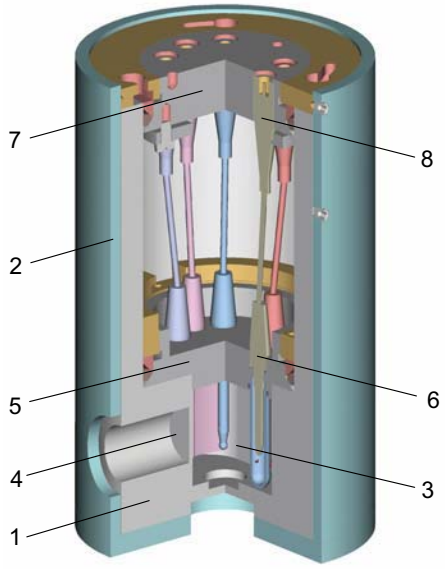

Fig. 1. Drawing of the spectro-electrochemical cell.

1 – Cell body of chemically resistant material
2 – Stainless steel housing
3 – Space for the sample solution
4 – X-ray window
5 – Inner cover plate (first compartment)
6 – Electrode
7 – Outer cover plate (second compartment)
8 – Electrical connector

Each cover plate contains six gas-tight connectors for cables and electrodes. Two X-ray windows were machined directly into the cell walls to avoid additional sealing. The windows are 20 mm apart from each other to allow sufficient X-ray transmission through the chloride solution and to achieve an edge jump of 0.3 at the U L_{III} edge.

The liquid volume of 10 ml was agitated by a magnetic stirrer. All miniaturized electrodes and sensors were machined by KSI Mainsberg and were used in combination with a potentiostat (model PGU 20V-100mA). The working electrode (cathode) was a Pt gauze and the counter electrode (anode) was an Ag wire.

The electrochemical reduction of U(VI) to U(IV) involves an electron transfer and a chemical reaction transforming the trans-dioxo cation. The reaction at the cathode is:

$$UO_2^{2+} + 2e^- + 2H^+ \rightarrow U^{4+} + 2H_2O. \quad (1)$$

At the anode silver is dissolved and precipitates as silver chloride:

$$2Ag + 2Cl^- \rightarrow 2AgCl\downarrow + 2e^-. \quad (2)$$

The dissolved Ag^+ ions are in equilibrium with solid AgCl and the equilibrium potential of the electrode is then determined by the solubility constant of the precipitate. At the experimental conditions chosen, the electrochemical potential was always far away from the decomposition potential of water. In order to avoid a high polarization of the cell, no diaphragm was used. The reduction of 0.01 moles of U(VI) to U(IV) at the cathode is accompanied by a decrease in the chloride concentration due to the precipitation of 0.02 moles of AgCl. The resulting reduction of the chloride concentration is small in comparison to the chloride concentration of the 3, 6 and 9 M Cl^- samples (see next paragraph). In order to enforce the anode reaction in the nominally 0 M Cl^- solution, 0.02 moles of LiCl were added. For both we did not expect an influence on speciation due to the low complex stability of uranium chloride ions. The Ag/AgCl potential was used as reference. Current-potential measurements were applied in order to gain redox potentials of the U(VI):U(IV) couple and appropriate potentials for the reduction process. XANES measurements were performed during the reduction process in situ to monitor the actual oxidation state. An example for the in situ XANES measurement comprising subsequent factor analysis is shown in Figure 2.

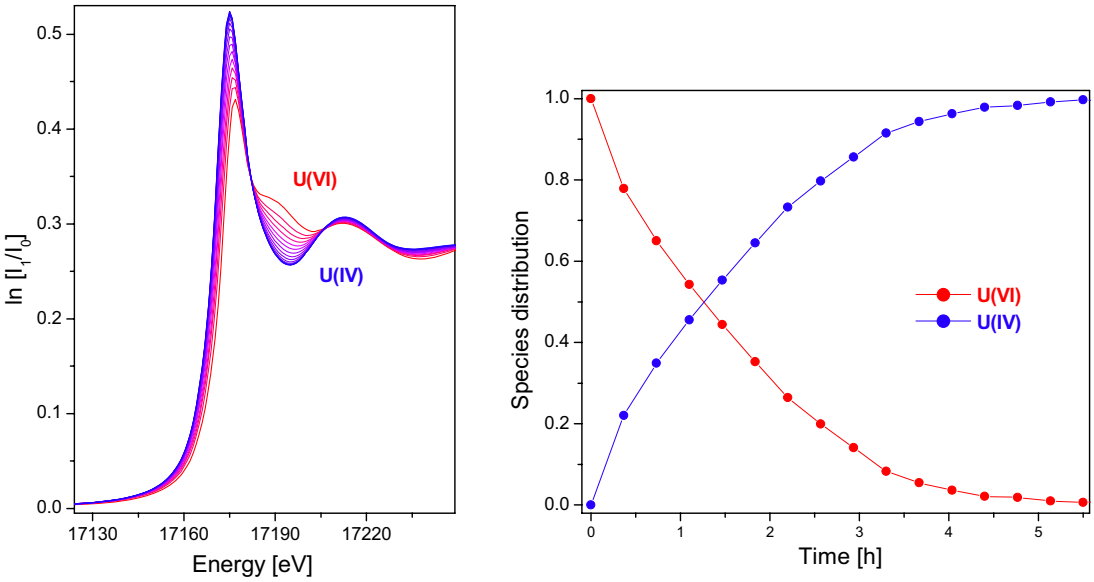

Fig. 2. *In situ* XANES measurements and species distribution in the solution. Left side: U L_{III} edge XANES spectra obtained during the reduction of 0.01M U(VI) in 0.2 M formic acid. The reduction was performed at a constant potential of –350 mV vs. Ag/AgCl. Right side: Distribution of U(VI):U(IV) species extracted by factor analysis.

Experimental

Two stock solutions of 0.1 M U were prepared by dissolving UO_3 either in 0.3 M $HClO_4$ for the chloride-free sample or in 0.3 M HCl for the chloride-containing samples. Four 0.01 M U(VI) aqueous solutions with chloride concentration of 0, 3, 6 and 9 M were prepared. LiCl was dissolved in 2.5 mL U stock solution and 2.5 mL of 1 M HCl obtaining 25 mL of 0.01 M U solutions.

Results and discussion

Comprehensive reviews of thermodynamic data have been reported on U(VI) complexes: a weighted linear regression, using experimental values from different references, yields stability constants of log β_1^0 = 0.17 ±0.02 and log β_2^0 = -1.1 ±0.02 for the reaction $UO_2^{2+} + nCl^- \rightleftharpoons UO_2Cl_n^{2-n}$ [1]. Formation constants log β_n^0 for species with n > 2 have not been published so far. UV-Vis spectroscopy shows significant spectral features which allowed to discriminate the species UO_2^{2+}, UO_2Cl^+ and $UO_2Cl_2^0$ quantitatively [2]. Allen et al. observed the species $UO_2(H_2O)_5^{2+}$, $UO_2(H_2O)_xCl^+$, $UO_2(H_2O)_xCl_2^0$, and $UO_2(H_2O)_xCl_3^-$ recently by EXAFS spectroscopy [3].

In contrast to U(VI), little is known on chloride complexation by U(IV). The formation constant according to the reaction $U^{4+} + nCl^- \rightleftharpoons UCl_n^{4-n}$ extrapolated to an ionic strength I = 0 yields log β_1^0 = 1.72 ±0.13 [1]. Only one experimental value is obtained for n = 2 with a log β_2 = 0.06 (I = 2 M) [4].

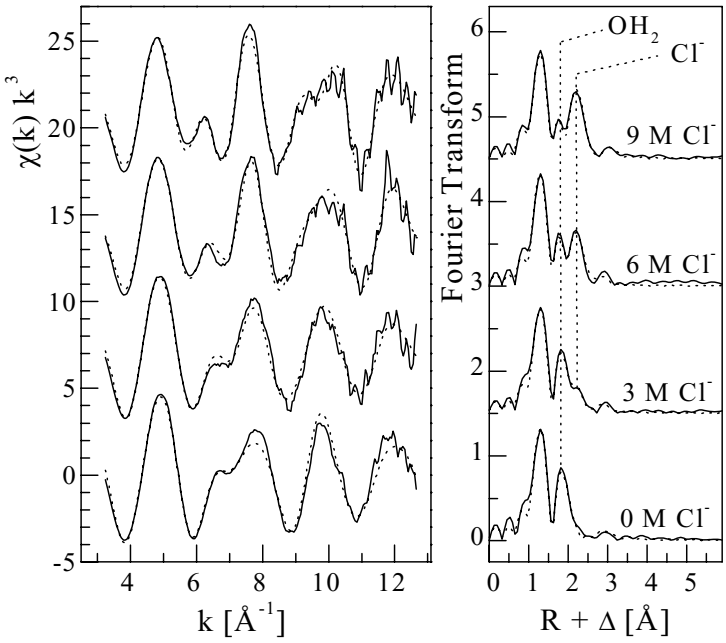

Fig. 3. U L_{III}-edge k^3 weighted EXAFS data (left) and corresponding Fourier transforms (right) taken over k = 3.2-12.7 Å^{-1} for UO_2^{2-} as a function of Cl^- concentration, experimental data (line) and theoretical curve fit (dots).

U L_{III}-edge k^3-weighted EXAFS spectra and the corresponding Fourier transforms (FT) of U(VI) samples are shown in Figure 3. The FT of all samples shows two peaks which arise from two axial oxygen atoms (O_{ax}) at 1.76 ±0.02 Å. The UO_2^{2+} aquo ion (sample 0 M Cl^-) shows 5 equatorial oxygen atoms (O_{eq}) at 2.41 ±0.02 Å. The FTs of the Cl^- solutions show an additional peak at a distance of 2.73 ±0.02 Å indicative of Cl^- in the first coordination sphere. The intensity of this Cl peak increases with increasing Cl^-

concentration. N_{Cl} increases from 1.0 to 2.7 in subsequent EXAFS fits. With increasing Cl^- concentration the dominant FT peak shifts to higher R values indicating a systematic replacement of H_2O by Cl^- in the first coordination sphere.

Possible solution species comprising $UO_2(H_2O)_5^{2+}$ and $UO_2(H_2O)_{5-n}Cl_n^{2-n}$ are averaged to a common radial distribution. However, the structural parameters extracted by EXAFS suggest the species $UO_2(H_2O)_4Cl^+$, $UO_2(H_2O)_3Cl_2^0$ and $UO_2(H_2O)_2Cl_3^-$ according to Figure 4.

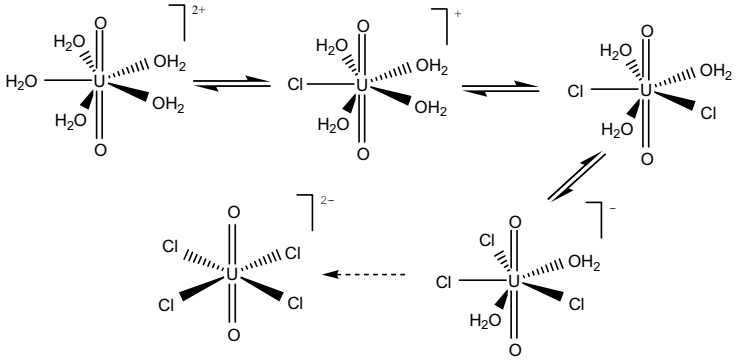

Fig. 4. U(VI) aquo chloro species.

We assume, that in all aquo chloro species the equatorial coordination number remains 5, because in a fourfold coordination as in $UO_2Cl_4^{2-}$ the U-Cl bond length would be reduced to 2.671 Å [5]. With increasing Cl^- concentration the coordination number of Cl increases stepwise. The ligands are coordinated in an inner-sphere fashion. A possible additional outer-sphere coordination could not be verified since EXAFS measurement is not sensitive for the backscattering signals at R+Δ > 3 Å under the used experimental conditions and the outer sphere coordination would most likely be too disordered to be detected.

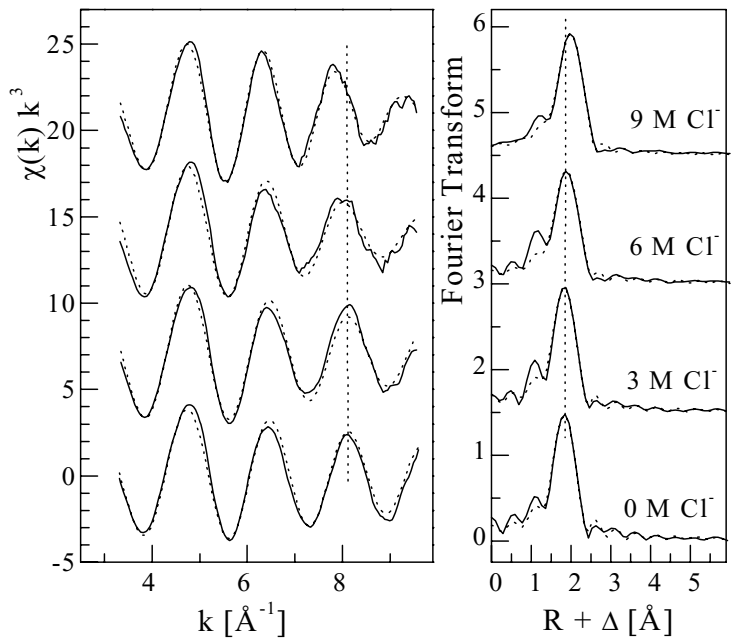

Fig. 5. U L_{III}-edge k^3 weighted EXAFS data (left) and corresponding Fourier transforms (right) taken over k = 3.2-9.6 $Å^{-1}$ for U(IV) as a function of Cl^- concentration, experimental data (line) and theoretical curve fit (dots).

Figure 5 shows the U L_{III}-edge k^3-weighted EXAFS spectra of U(IV). In non-complexing perchloric acid the U(IV) aquo ion shows 8.7 spherically arranged oxygen atoms at a distance of 2.41 Å.

With increasing Cl^- concentration the dominant FT peak shifts to higher R values indicating a systematic replacement of H_2O by Cl^- in a distance of 2.71 Å. During the fits, the σ^2 value of the U-O shell was fixed to 0.0070 $Å^{-2}$, obtained from the U(IV) aquo ion, and that of the U-Cl shell was fixed to 0.0050 $Å^{-2}$ following the value obtained for U(VI). The coordination number N_{Cl} increases from 0.3 to 2.1 and the coordination number N_O decreases from 8.5 to 6.1. The aquo chloro species derived from EXAFS measurements are identified as $U(H_2O)_8Cl^{3+}$, $U(H_2O)_{6\text{-}7}Cl_2^{2+}$ and $U(H_2O)_5Cl_3^{+}$ as shown in Figure 6. The extraction of principal components by factor analysis shows that the coordination number N_{O+Cl} decreases from 9 in $U(H_2O)_8Cl^{3+}$ to 8 in $U(H_2O)_5Cl_3^{+}$.

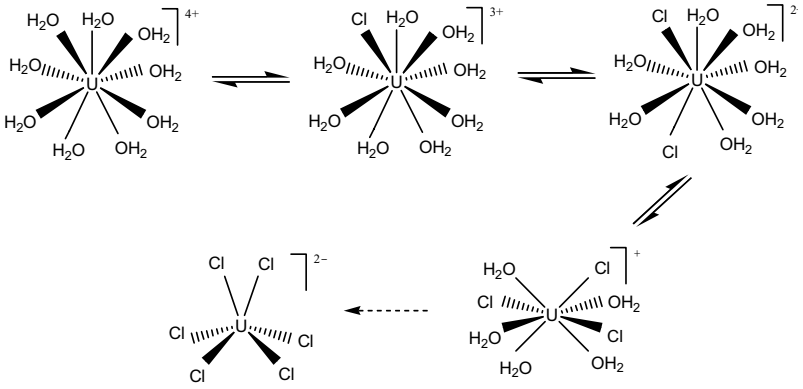

Fig. 6. U(IV) aquo chloro species.

The structure of U(IV) chloride complexes was not investigated up to now. Allen et al. [3] found clear evidence for inner-sphere formation of Np(IV) aquo chloride complexes. Due to the chemical similarity of U(IV) and Np(IV) an equivalent coordination was assumed for U(IV). A comparison of the Cl^- concentrations necessary to reach a coordination number of $N_{Cl} < 1$, which is higher for U(IV) than for Np(IV), confirms that log β_1 follows the trend U(IV) > Np(IV). The similar bond lengths for U-O and U-Cl for the U(VI) and U(IV) aquo chloro species suggests that, despite the difference in formal oxidation state, the effective ionic radii of U(VI) and U(IV) are similar, as has been pointed out in the literature [5].

Acknowledgements

The EXAFS measurements were performed at the Rossendorf Beamline/ESRF. We thank D. Rettig and T. Reich for technical development of a first version and furthermore J. Claußner and D. Falkenberg for their support of the final development of the spectro-electrochemical cell.

References

[1] Grenthe, I.; Fuger, J.; Konings, R.J.M.; Lemire, R.J.; Muller, A.B.; Nguyen-Trung, C.; Wanner, H. In *Chemical Thermodynamics of Uranium*; Wanner, H.; Forest, I., Eds.; Elsevier Science Publishers: Amsterdam, 1992, p. 192.

[2] Paviet-Hartmann, P.; Lin, M.R., *Mat. Res. Soc. Symp. Proc.* 1999, *556*, 977-984.

[3] Allen, P.G.; Bucher, J.J.; Shuh, D.K.; Edelstein, N.M.; Reich, T. *Inorg. Chem.* 1997, *36*, 4676-4683.

[4] Day, R.A., Jr.; Wilhite, R.N.; Hamilton, F.D., *J Am. Chem. Soc.* 1955, *77*, 3180-3182
[5] Watkin, D.J.; Denning, R.G.; Prout, K. *Acta Cryst.* 1991, *C47*, 2517-2519
[6] Denning, R.G. Electronic structure and bonding in actinyl ions, In *Structure and Bonding*, Vol. 79, Springer, Heidelberg 1992.